Drug Design, Development and Therapy

Dovepress
Taylor & Francis Group

Open Access Full Text Article

ORIGINAL RESEARCH

Emodin Alleviates Monocrotaline-Induced Pulmonary Arterial Hypertension by Directly Targeting TAK1

Yaolei Zhang[1,2], Mingmei Zhang[3], Ting Li[2], Yunchuan Liu[1], Zihan Li[4], Longfu Zhou[5], Yonghe Hu[1,4]

[1]School of Materials Science and Engineering, Southwest Jiaotong University, Chengdu, People's Republic of China; [2]Clinical Biobank Center, General Hospital of Western Theater Command, Chengdu, People's Republic of China; [3]Department of Rheumatology and Immunology, General Hospital of Western Theater Command, Chengdu, People's Republic of China; [4]College of Medicine, Southwest Jiaotong University, Chengdu, People's Republic of China; [5]Department of Biomedical Engineer, General Hospital of Western Theater Command, Chengdu, People's Republic of China

Correspondence: Yonghe Hu, School of Materials Science and Engineering, Southwest Jiaotong University, No. 111, North Section 1, Second Ring Road, Chengdu, Sichuan, 610031, People's Republic of China, Tel +86 028-86571619, Email yonghehu123@163.com

Drug Design, Development and Therapy downloaded from https://www.dovepress.com/
For personal use only.

Purpose: Pulmonary arterial hypertension (PAH) is a group of diseases characterized by elevated pulmonary arterial pressure. The malignant proliferation of pulmonary artery smooth muscle cells is a major pathological hallmark of PAH. Emodin, a natural compound with known antiviral, anti-inflammatory, and anti-proliferative properties, has shown potential in alleviating PAH. Our aim is to elucidate the core pathways and molecular targets through which emodin exerts its therapeutic effects in alleviating PAH.

Methods: Firstly, potential targets of emodin in alleviating PAH were predicted using network pharmacology. Molecular docking was used to predict the binding affinity between emodin and its targets, and the interactions between emodin and these targets were verified using the Cellular Thermal Shift Assay, Co-immunoprecipitation, and Immunofluorescence. Ultrasound and pathological analyses were employed to evaluate the effects of emodin on monocrotaline-induced PAH. Finally, the results obtained from network pharmacology were validated using hematoxylin and eosin staining, ultrasound imaging, Western blotting, and polymerase chain reaction.

Results: Emodin relieves PAH by inhibiting PASMC proliferation, reducing right ventricular hypertrophy, and decreasing lung inflammation. It targets eight proteins in 15 pathways, including IL-17 signaling. Molecular docking shows emodin binds to key IL-17 pathway molecules, reducing IL-17A, IL-17RA, and Phospho-TAK1 expression. Emodin binds competitively to TAK1, preventing its interaction with MKK3, inhibiting TAK1 phosphorylation and downstream pathway activation, thus suppressing inflammation. The indispensable role of TAK1 in mediating emodin's effects was corroborated through pharmacological blockade with Takinib, a highly potent and selective TAK1 inhibitor.

Conclusion: The experiment has demonstrated for the first time that emodin directly targets TAK1, downregulates the expression of IL-17A, IL-17RA, and Phospho-TAK1, blocks the activation of the IL-17 signaling pathway, inhibits PASMCs proliferation, and alleviates PAH. This study provides a theoretical basis for the clinical application of emodin.

Keywords: emodin, pulmonary arterial hypertension, network pharmacology, TAK1, IL-17 signaling pathway

Introduction

With the changes in people's diet and lifestyle in modern society, the incidence of Pulmonary arterial hypertension (PAH) is increasing annually and becoming more prevalent among younger populations.[1] Beyond progressive respiratory insufficiency, PAH invariably precipitates systemic sequelae, most notably pathological right-ventricular hypertrophy that frequently advances to overt right-sided heart failure.[2] Against this dire backdrop, the expeditious development of an efficacious therapeutic intervention has emerged as an exigent and unmet clinical imperative. Currently, commonly used drugs for PAH in clinical practice, such as calcium channel blockers and anticoagulants, have certain therapeutic effects but are associated with significant adverse reactions and side effects upon long-term use.[3] Targeted drugs, including bosentan and tadalafil, have demonstrated notable efficacy; however, issues related to adverse reactions and potential

Received: 6 June 2025
Accepted: 24 September 2025
Published: 30 September 2025

© 2025 Zhang et al. This work is published and licensed by Dove Medical Press Limited. The full terms of this license are available at https://www.dovepress.com/terms.php and incorporate the Creative Commons Attribution – Non Commercial (unported, v4.0) License (http://creativecommons.org/licenses/by-nc/4.0/). By accessing the work you hereby accept the Terms. Non-commercial uses of the work are permitted without any further permission from Dove Medical Press Limited, provided the work is properly attributed. For permission for commercial use of this work, please see paragraphs 4.2 and 5 of our Terms (https://www.dovepress.com/terms.php).

Graphical Abstract

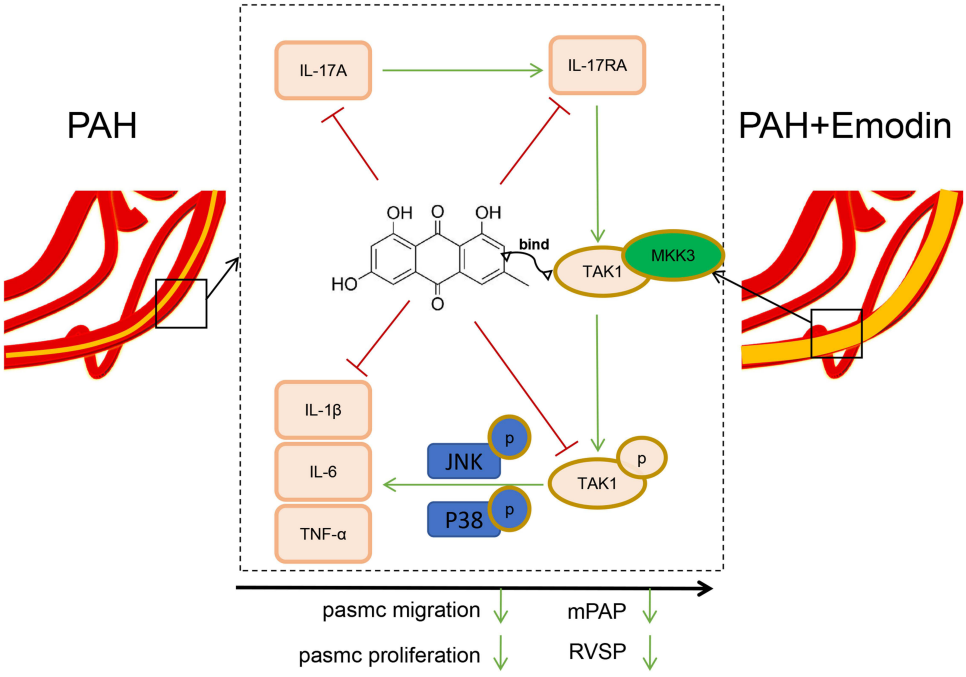

liver and kidney damage remain unresolved.[4] Therefore, the need to identify a safe and effective therapeutic agent is extremely urgent.

Quantitative experiments have shown that the malignant proliferation of pulmonary artery smooth muscle cells (PASMCs) is a critical factor in the progression of PAH.[2] Thus, effectively inhibiting the proliferation of PASMCs has become a focal point in current research. As a systemic disease, PAH is directly promoted by the malignant proliferation and anti-apoptotic phenotype exhibited by PASMCs,[5] Elevated levels of IL-6 and IL-1β in the blood have been identified in PAH patients,[6] Our previous studies demonstrated that inhibiting the inflammatory response mediated by NF-κB can attenuate the progression of PAH,[7] Additionally, bone morphogenetic protein receptor II and bone morphogenetic protein 9 have been implicated in the regulation of cell apoptosis and the development of PAH.[8,9] Emodin, an anthraquinone derivative, has garnered significant attention for its antioxidant, anti-tumor, and anti-inflammatory properties.[10] Our research team previously reported that emodin significantly inhibits reactive oxygen species (ROS) generation, alleviates vascular oxidative stress damage, and suppresses the malignant proliferation of PASMCs, suggesting its potential as a vascular smooth muscle cell proliferation inhibitor.[11] Consistent with these findings, other studies have shown that emodin inhibits TNF-α-induced proliferation of human aortic smooth muscle cells via mitochondrial-dependent apoptosis.[12] Emodin has been reported to inhibit the viability, proliferation, and migration of pulmonary artery smooth muscle cells under hypoxic conditions by regulating miR-244-5p, promoting cell apoptosisEmodin has also been reported to inhibit the viability, proliferation, and migration of PASMCs under hypoxic conditions by regulating miR-244-5p and promoting cell apoptosis.[13] Furthermore, emodin may inhibit AngII-induced proliferation of vascular smooth muscle cells (VSMCs) by suppressing c-myc expression.[14] Collectively, these findings suggest that emodin may play a significant role in alleviating PAH; however, the underlying mechanisms remain to be elucidated.

Due to the multiple targets and complex mechanisms of emodin,[15] the effect of emodin on PAH cannot be fully elucidated through the study of a single component. Network pharmacology has emerged as a powerful tool for elucidating the mechanisms of drug therapy, particularly in its ability to address multi-target and multi-pathway characteristics.[16,17] In this study, we employed network pharmacology approaches to identify potential targets of emodin

in alleviating PAH and combined these findings with animal model verification to elucidate the mechanisms underlying emodin's therapeutic effects on PAH.

Materials and Methods

Establishment of Animal Models

All animal experiments were performed in accordance with the National Institutes of Health Guide for the Care and Use of Laboratory Animals and were approved by the Animal Research Ethics Committee of The General Hospital of Western Theater Command (Chengdu, China) and complied with the Guidelines for Animal Experiments (Ethical approval number: 2025EC1-ky013). Thirty male rats, aged 6 weeks and weighing 180–200 g, were purchased from Chengdu Dashuo Biotechnology Co., Ltd. (China; license no. SCXK [chuan] 2020–0030). All mice were housed in a controlled environment (12 h light/dark cycle, temperature 22 ± 2°C, humidity 50 ± 10%), allowed free access to water and food, and acclimated for at least 7 days prior to surgery. Rats were randomly divided into five groups (n = 6 per group) using the random number table method: control group, emodin group, MCT group, MCT+emodin group, and MCT+emodin+Takinib group. PAH was induced by a single subcutaneous injection of monocrotaline (MCT; C2401, Sigma, USA; 60 mg/kg),[5] while the control group was injected with an equal amount of solvent. The emodin group emodin was only orally administered with emodin (70mg/kg, HY-14393, MCE, USA) for 21 days. The MCT+Emodin group was orally administered with Emodin (70mg/kg) for 21 days after injection of MCT. The MCT+Emodin+Takinib group was orally administered with Emodin (70mg/kg) and Takinib (50mg/kg, EDHS-206, MCE, USA) for 21 days after injection of MCT. The control group received an equivalent volume of vehicle. After the final administration, all rats were fasted for 12 hours and subjected to echocardiography analysis. Subsequently, rats were anesthetized with 3% pentobarbital sodium, and serum was collected. Lung and heart tissues were harvested, snap-frozen in liquid nitrogen, and stored at −80°C for further biochemical analysis. A portion of the lung tissue was fixed in 4% paraformaldehyde (BL539A, Biosharp, China) for histological examination.

Small Animal Ultrasound

Cardiac ultrasound was performed to assess changes in pulmonary artery pressure and right ventricular wall thickness in each experimental group. First, the chest hair of the rats was removed to facilitate probe contact. Right ventricular images were captured using a Vevo3100 ultrasound system (FUJIFILM Visual Sonics, Toronto, ON, Canada) equipped with a 400 MHz probe in M-mode. The following parameters were measured using the system's software: Diastolic right ventricular free wall thickness (RVFWT), End diastolic right ventricle diameter (RVEDD). The probe was then rotated to the optimal position for measuring pulmonary artery blood flow, where the following parameters were assessed: Mean pulmonary artery pressure (mPAP), Pulmonary artery acceleration time (PAT), Pulmonary artery ejection time (PET). All data were analyzed using Vevo LAB offline analysis software (Version 5.5.1).

Right Heart Floating Catheter for Detecting Pulmonary Artery Pressure

Rats were anesthetized by intraperitoneal injection of sodium pentobarbital (40 mg kg^{-1}, i.p.) and subsequently placed in a supine position with limbs secured to the operating platform. The right external jugular vein was fully exposed, with the distal end ligated and a flexible knot tied near the proximal end. A pressure catheter (Millar Instruments) equipped with a micropressure gauge tip was inserted through the right external jugular vein into the right ventricle and advanced until it reached the pulmonary artery.The mPAP and RVSP were recorded using the PowerLab system (ADInstruments), a high-performance data acquisition platform designed for precise and reliable hemodynamic measurements. Data were analyzed using LabChart software (Version 8.1.30), which provides a comprehensive platform for acquiring and analyzing biological signals. The analysis was based on established protocols and previous literature.[18]

Hematoxylin and Eosin (H&E) Staining

Lung and heart tissues were fixed in 4% paraformaldehyde for 24 hours, followed by routine dehydration and paraffin embedding. Sections (4 μm) were prepared and dewaxed in xylene, then rehydrated through a graded ethanol series

(100%, 95%, 80%, and 70% ethanol) to distilled water. The H&E staining kit (BL700B, Biosharp, China) was used to stain the sections according to the manufacturer's instructions. Stained sections were then photographed using a light microscope.[19]

Serum Inflammatory Factor Detection

The concentrations of IL-1β (JL18442), IL-6 (JL20268), and TNF-α (JL10484) in rat serum were measured using ELISA kits from JONLNBIO (China). The assays were performed according to the manufacturer's instructions.[19]

Drug Target Screening

The target sites of emodin were identified through the Traditional Chinese Medicine Systems Pharmacology (TCMSP) database (http://tcmspw.com/tcmsp.php). The relevant target sites associated with PAH were queried using the DisGeNET database (https://www.disgenet.org/) and GeneCards database (https://www.genecards.org/). The overlapping analysis between the targets of emodin and those related to PAH was performed using the Venny 2.1 tool (https://bioinfogp.cnb.csic.es/tools/venny/).

Protein-Protein Interaction Analysis

The overlapping genes identified in the previous step were introduced into the STRING database (https://string-db.org/) to construct a protein-protein interaction (PPI) model. The PPI network was visualized using Cytoscape software, which allowed for the analysis of interactions among the proteins associated with the identified targets.

Component-Target-Disease Network

The components, overlapping targets, and related diseases were imported into Cytoscape 3.9.1 to construct a composite target network. Visualization processing was performed simultaneously to analyze the relationships among the components, targets, and diseases. This network provides a comprehensive overview of the interactions and connections within the system, facilitating the identification of key nodes and pathways involved in the therapeutic effects.

Gene Ontology (GO) and Pathway Enrichment

The interaction relationships between overlapping targets and biological pathways were analyzed using the DAVID 2021 database (https://david.ncifcrf.gov/). The identified target genes were imported into DAVID for GO analysis and KEGG pathway enrichment analysis. The results were processed for visualization to elucidate the functional annotations and pathway associations of the target genes.

Molecular Docking

To further understand the binding ability of emodin to its key target, molecular docking experiments were conducted. Firstly, the three-dimensional (3D) structure of emodin was obtained from ChemDraw, and its energy was minimized using ChemOffice software. The 3D structure of the receptor was retrieved from the Protein Data Bank (PDB) database (https://www.rcsb.org/). After removing water molecules, deoxysugars, and hydrogen atoms using PyMOL software, the receptor and ligand structures were converted into PDBQT format using AutoDockTools 1.5.6. Molecular docking simulations were performed using the AutoDock Vina platform. The conformation with the best binding affinity was selected as the final docking conformation. Visualization of the docking results was carried out using PyMOL software. The specific method was adapted from a previously published article.[19]

Cell Experiment

PASMCs were purchased from Shanghai Yubo Biotechnology Co., Ltd. The cells were cultured in High Glucose DMEM (Hyclone) supplemented with 10% fetal bovine serum (FBS; Gibco) and 1% Penicillin-Streptomycin Solution (Hyclone). Cells were maintained at 37°C in a humidified incubator with 5% CO_2. Angiotensin II (AngII, 4 μM) was used to induce the proliferation of PASMCs for 24 or 48 hours.[20] Other experimental procedures were consistent with previously published methods.[21]

Cell Counting Kit-8 (CCK8) Assay

PASMCs were seeded at a density of 8000 cells per well in 96-well plates and divided into eight groups. The control group received no treatment with Ang II or emodin. The Ang II group was treated with Ang II (20 μM), while the Ang II + Emodin groups were treated with Ang II (20 μM) in combination with various concentrations of emodin (3.1 μM, 6.3 μM, 12.5 μM, 25 μM, 50 μM, and 100 μM). After 24 h and 48 h of treatment, the original culture medium was removed, and 110 μL of CCK8 working solution (10 μL CCK8 stock solution + 100 μL High Glucose DMEM) was added to each well. The cells were then incubated for an additional 2 h. The absorbance at 450 nm was measured using a microplate reader (Thermo), and the proliferation rates of each group were calculated based on the absorbance values.

Cell Scratch Assay

PASMCs were cultured in 6-well plates until they reached confluence. A scratch was made in the monolayer using a sterile pipette tip, and cell debris was removed by washing with PBS. The cells were then cultured in serum-free medium. Except for the control group, the other two groups were treated with Ang II (20 μM). Additionally, the Ang II + Emodin group received emodin (20 μM). Images of the scratch wounds were captured at 0 h and 24 h using an optical microscope (DMLB2, Leica, Germany). The migration distances of the cells in each group were measured using Image Pro Plus software.

Tunel Staining

PASMCs were cultured in 6-well plates until they reached 80% confluence. Except for the control group, the other groups were treated with Ang II (20 μM). The Ang II + Emodin group received an additional treatment with emodin (20 μM). After 24 hours, the cells were fixed with 4% paraformaldehyde for 30 minutes at room temperature. The Fluorescein TUNEL Cell Apoptosis Detection Kit (G1501, Servicebio, China) was used according to the manufacturer's instructions. Images were captured under a fluorescence microscope (Olympus, IX81, Japan) using a FITC filter to visualize the green fluorescence indicative of apoptotic cells. The apoptosis rate was calculated using Image Pro Plus software by quantifying the number of TUNEL-positive cells relative to the total number of cells.

Immunohistochemistry

Tissue samples were routinely dehydrated and embedded, sectioned at 4 μm, dewaxed, and rehydrated. The sections were placed in an acid repair solution (BL619A, Biosharp, China) at 100 °C for 2 minutes to enhance antigen retrieval. Endogenous peroxidase activity was blocked by incubating the sections with 3% H_2O_2 for 10 minutes. Sections were then incubated with goat serum (AR1009, BOSTER, China) for 10 minutes to prevent nonspecific binding. Primary antibody against α-SMA (67735-1-lg, Proteintech, USA) was added at a dilution of 1:200 and incubated overnight at 4 °C. Other steps were performed according to previously published methods.[19]

Western Blot (WB)

Lung tissue and PASMCs total protein were pre-treated according to previously published methods. The content of target proteins was detected by SDS-PAGE gel electrophoresis. Primary Antibodies: anti-IL-17A (ab318150, Abcam, UK), anti-IL-17RA (ab318130, Abcam, UK), anti-TAK1 (ab109526, Abcam, UK), anti-Phospho-TAK1 (bs-5435R, Bioss, China), anti-GAPDH (bs-10900R, Bioss, China), anti-JNK1/2 (9252, CST, USA), anti-Phospho-JNK1/2 (4668, CST, USA), anti-p38 (8690, CST, USA), anti-Phospho-p38 (8690, CST, USA), anti-MKK3 (R24950, Zenbio, China). Secondary antibodies: Goat anti-rabbit (GB23303, Servicebio, China), Goat anti-mouse (GB23301, Servicebio, China). The remaining steps were performed according to previously published methods.[19]

Co-Immunoprecipitation

PASMCs were transfected with Flag-labeled TAK1 (Flag-TAK1), and then treated with emodin at the specified concentration for 6 hours. Cells were lysed using Western blotting and IP cell lysis buffer (R0100, Solarbio). Meanwhile, Protein Phosphatase Inhibitor (P1260, Solarbio) was added. Centrifuge the lysis buffer at 14,000 rpm for

10 min and discard the cell debris. For immunoprecipitation, the cell lysates were incubated with monoclonal anti-HA agarose, Anti-FLAG M2 affinity gel, or the corresponding antibody overnight at 4 °C. The immunoprecipitate was analyzed by WB.

Cellular Thermal Shift Assay (CETSA)

PASMCs were seeded in 10 cm culture dishes. After reaching 80% confluence, emodin (20 μM) was added to the Emodin group, while an equivalent volume of DMSO was added to the control group. After 6 h, the cells were washed three times with PBS, digested with trypsin, and resuspended in 1 mL of PBS containing protease and phosphatase inhibitors. The cell suspension was divided into four equal parts (250 μL each) and transferred to EP tubes. The samples were heated at 40°C, 50°C, 60°C, and 65°C for 5 minutes, respectively, followed by cooling at room temperature for 3 minutes. The cells were then subjected to repeated freeze-thaw cycles and centrifuged at 12,000 rpm for 10 minutes to collect the supernatant. The supernatant was mixed with loading buffer, boiled for 10 minutes, and stored at −20°C. Western blotting was performed to detect the expression changes of IL-17A, IL-17RA, TAK1, and phospho-TAK1. Specific operational steps were performed according to previously published methods.[19]

Quantitative Real Time-Polymerase Chain Reaction (PCR)

Total RNA was extracted from lung tissues using a standard RNA extraction kit. Specific primers were designed and synthesized by Sangon (China) (Table 1). Specific operational steps were performed according to previously published methods.[19]

Statistical Analysis

Experimental data were analyzed using SPSS 25.0 software. Data were first subjected to a normality test. For normally distributed data, one-way ANOVA was used for multiple group comparisons, or an unpaired two-tailed Student's *t*-test was used for comparisons between two groups. For data that did not follow a normal distribution, the Kruskal–Wallis test was applied. Statistical significance was set at $p = 0.05$. Differences were marked as follows: $*p < 0.05$, $**p < 0.01$, $***p < 0.001$, and ns ($p > 0.05$) for non-significant results.

Results

Potential Targets of Emodin for Alleviating PAH

Using network pharmacology, we identified the target sites of emodin and those associated with PAH. Our analysis revealed that emodin has 35 effective targets, while PAH has 156 relevant targets. Through Venn diagram intersection analysis, we identified 8 potential interaction targets between emodin and PAH (Figure 1A). The PPI network illustrates

Table 1 Primers Which Have Been Used for Real Time PCR

Primer name	Sequence 5'-3'	Product length
IL-17A	Forward: CTACCTCAACCGTTCCACTT Reverse: ACTTCTCAGGCTCCCTCTTC	191 bp
IL-17RA	Forward: ATCTTGCCAACAACAGACCTGACTC Reverse: GACGATGATCTTGGAACCGCTCTC	246 bp
TAK1	Forward: CGCCATCGCAGGTCCTTAACTTC Reverse: GCCTCCTTCAGCATACTCCATCAC	269 bp
IL-1β	Forward: CCACAGACCTTCCAGGAGAA Reverse: GTGATCGTACAGGTGCATCG	121 bp
IL-6	Forward: ACTTCACAAGTCGGAGGCTT Reverse: AGTGCATCATCGCTGTTCAT	107 bp
TNF-α	Forward: GGTGATCGGTCCCAACAAGGA Reverse: CACGCTGGCTCAGCCACTC	173 bp
GAPDH	Forward: AGTGCCAGCCTCGTCTCATA Reverse: GGTAACCAGGCGTCCGATAC	77 bp

the interactions and relationships among these targets. The 8 target nodes are interconnected by 22 edges, with an average node degree of 5.5, an average local clustering coefficient of 0.87, an expected number of edges of 8, and a PPI enrichment p-value of 5.87E-05 (Figure 1B). These 8 hub genes are TNF, PTGS2, MMP1, MMP9, MYC, SLC2A4, CYP1A1, and PPARG. Visualization using Cytoscape shows that the darker and larger the node, the more crucial the protein is likely to be in the therapeutic effects of emodin on PAH (Figure 1C). These results suggest that emodin may play a significant role in the pathogenesis and progression of PAH through interactions with these key targets.

Emodin Alleviates PAH and Myocardial Remodeling

Small animal ultrasound and right heart floating catheterization were used to assess changes in PAH and right ventricular wall thickness.[22] Results showed that compared with the control group, emodin treatment alone did not significantly affect mPAP, RVSP, PAT, or PAT/PET ratio ($p > 0.05$). In the model group induced by MCT, mPAP was significantly increased ($p < 0.01$), while PAT and PAT/PET were significantly decreased ($p < 0.01$) (Figure 2A–E). Emodin intervention significantly reduced mPAP and RVSP ($p < 0.01$) and increased PAT and PAT/PET compared to the model group ($p < 0.01$) (Figure 2A–E). Right ventricular wall thickening is a severe complication of PAH. Ultrasound results showed that emodin administration did not affect RVFWT or RVEDD compared to the control group ($p > 0.05$) (Figure 2F–H). However, MCT-induced PAH led to significant increases in RVFWT and RVEDD ($p < 0.01$) (Figure 2F–H). Emodin treatment effectively alleviated myocardial remodeling caused by MCT, as evidenced by reduced RVFWT and RVEDD compared to the model group ($p < 0.05$) (Figure 2F–H). These results suggest that emodin can effectively alleviate PAH and myocardial remodeling. However, the specific role of vascular smooth muscle cells in these effects remains to be elucidated.

Emodin Inhibits Malignant Proliferation of Pulmonary Artery Smooth Muscle Cells and Right Ventricular Hypertrophy

Histopathological changes in heart and lung tissues were assessed using H&E staining. The H&E results of heart sections showed that emodin intervention did not significantly affect myocardial remodeling or the right ventricle to left ventricle plus septum ratio (RV/(LV + S)) ratio compared to the control group ($p > 0.05$) (Figure 3A and B).

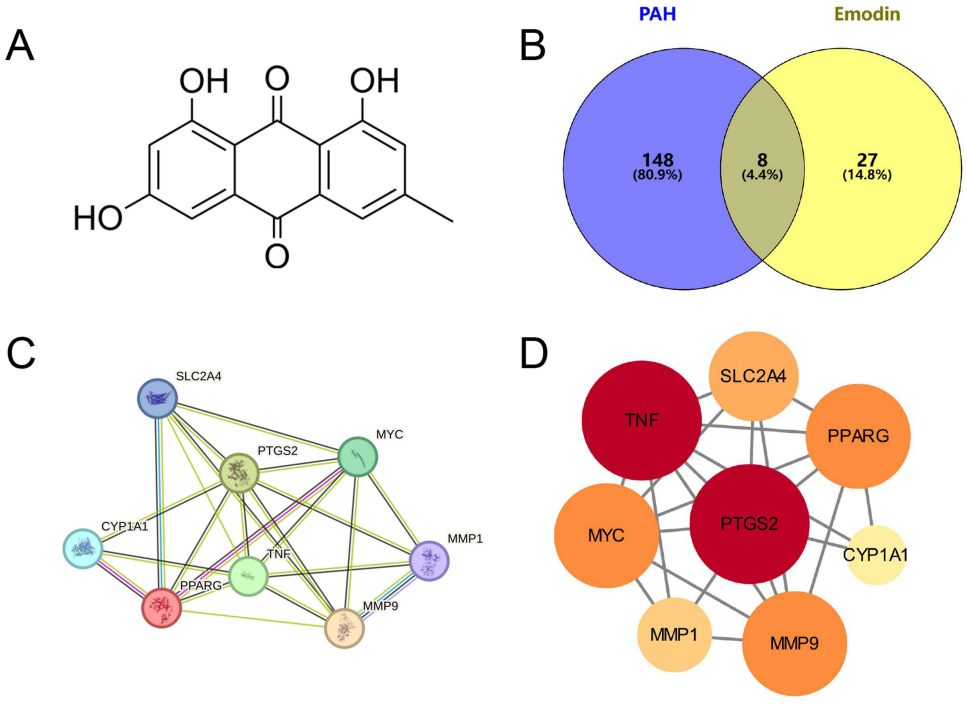

Figure 1 Potential targets and interaction relationships of emodin in alleviating PAH. (**A**) Structural formula of emodin. (**B**) Venn diagram showing the overlapping gene targets between emodin and PAH. (**C**) PPI network illustrating the relationships among the target proteins. (**D**) Visualization highlighting the importance of different targets, with darker and larger nodes indicating more critical proteins in the therapeutic effects of emodin.

https://doi.org/10.2147/DDDT.S540915

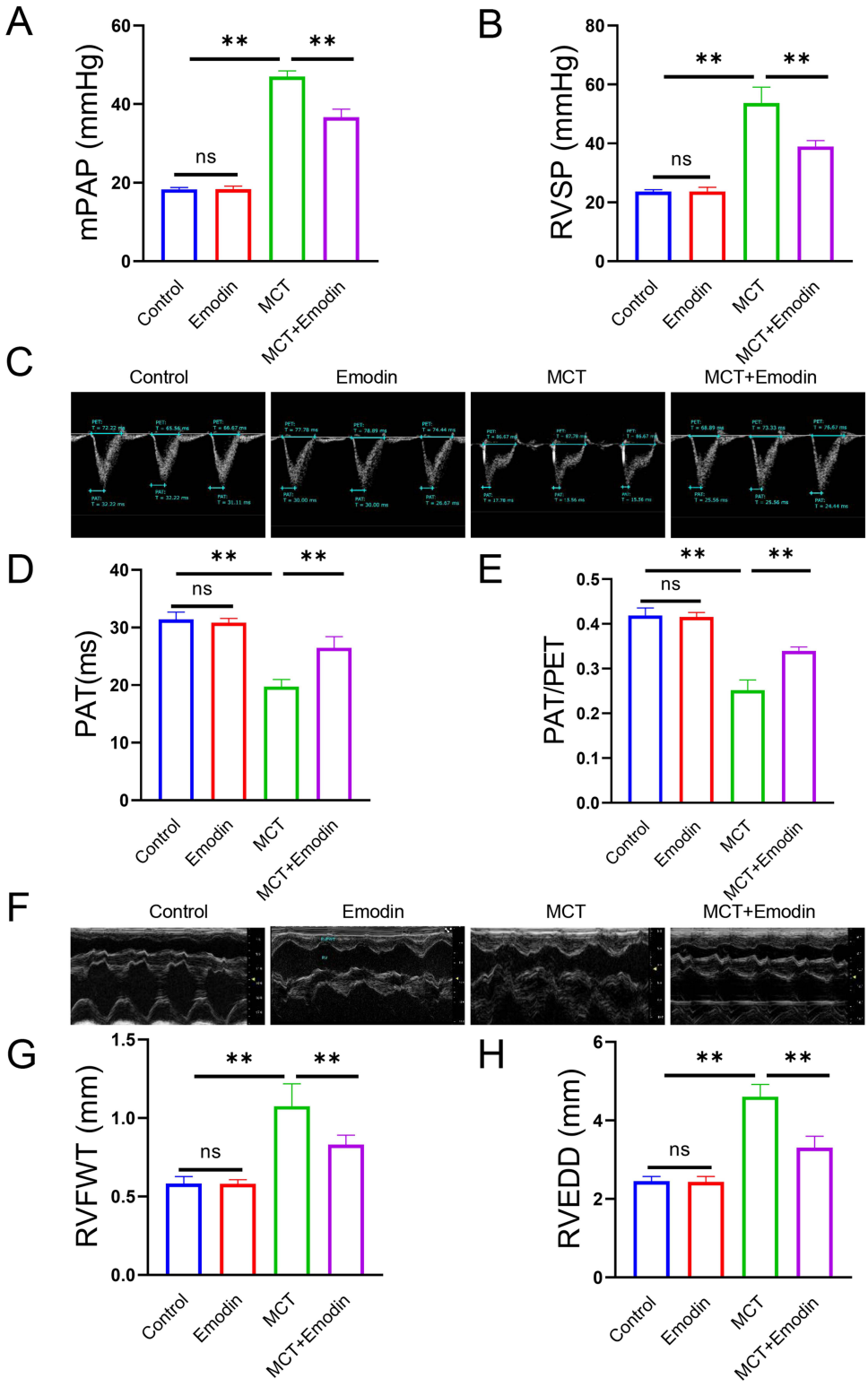

Figure 2 Emodin alleviates PAH and myocardial remodeling. Changes in mPAP (**A**) and RVSP (**B**) in each group. (**C**) Changes in pulmonary artery blood flow velocity measured by ultrasound in each group. Changes in PAT (**D**) and PAT/PET (**E**) in each group. (**F**) Trajectory of right ventricular and right atrial wall motion measured by ultrasound in each group. Changes in RVFWT (**G**) and RVEDD (**H**) in each group. The data are expressed as the mean ± standard deviation (±S).
Note: $^{**}p < 0.01$; ns $p > 0.05$.

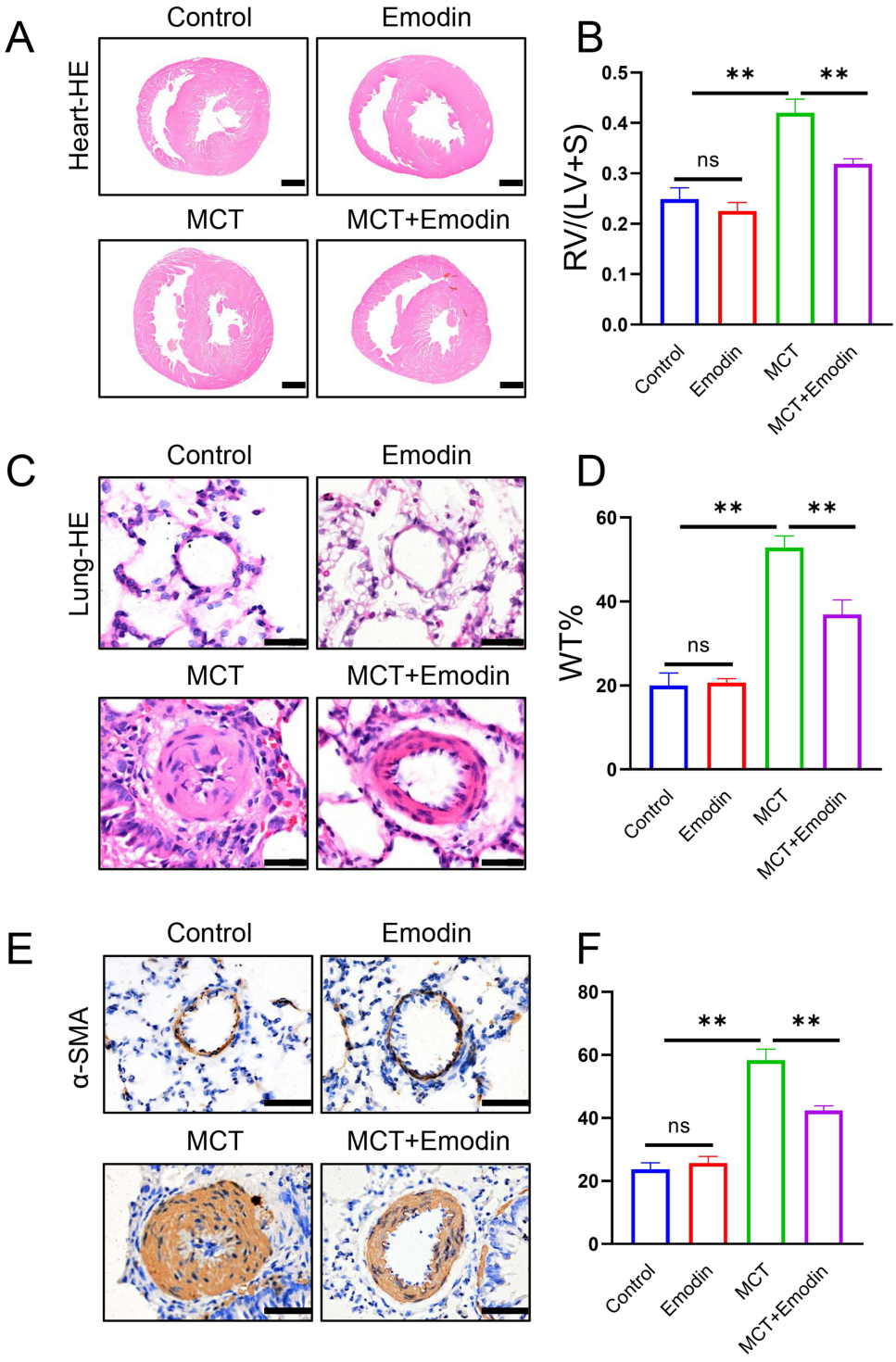

Figure 3 Emodin inhibits malignant proliferation of PASMCs and right ventricular hypertrophy. (**A**) H&E staining for pathological changes in in heart sections of each group. (**B**) Changes in RV/(LV + (**S**) ratio in each group. (**C**) H&E staining for pathological changes in pulmonary arteries in each group. (**D**) Changes in WT% in each group. (**E**) Immunohistochemical staining of PASMCs. (**F**) Changes in muscularization ratio of pulmonary arteries in each group. The data are expressed as mean ± standard deviation (±S).
Note: **$p < 0.01$; ns $p > 0.05$.

Consistent with the ultrasound findings, MCT-induced pulmonary hypertension led to significant cardiac remodeling, ventricular wall thickening, and an increased RV/(LV + S) ratio compared to the control group ($p < 0.01$) (Figure 3A and B). Emodin intervention significantly improved myocardial remodeling, relieved ventricular wall thickening, and decreased the RV/(LV + S) ratio compared to the MCT group ($p < 0.01$) (Figure 3A and B). The H&E results of lung

https://doi.org/10.2147/DDDT.S540915

tissue showed no significant changes in the emodin intervention group compared to the control group ($p > 0.05$) (Figure 3C). In the MCT group, inflammatory cell infiltration around the pulmonary arteries and significant thickening of the pulmonary artery lumen were observed ($p < 0.01$) (Figure 3C). Emodin intervention significantly reduced pulmonary inflammation and widened the pulmonary artery lumen compared to the MCT group ($p < 0.01$) (Figure 3C). The medial thickness percentage (WT%) was significantly improved after emodin intervention (Figure 3D). Although emodin significantly inhibited MCT-induced proliferation of PASMCs, the specific role of these cells in this process remained unclear. We labeled PASMCs with α-smooth muscle actin (α-SMA) (Figure 3E) and found that the thickened pulmonary artery lumen in MCT-induced pulmonary hypertension was primarily composed of smooth muscle cells. Compared to the MCT group, emodin significantly inhibited the malignant proliferation of PASMCs ($p < 0.01$) (Figure 3F). These results suggest that emodin alleviates MCT-induced PAH by inhibiting the malignant proliferation of PASMCs. However, the specific mechanisms underlying these effects remain to be elucidated.

Network Pharmacology Analysis of the Effect of Emodin on PAH

Network pharmacology offers significant advantages in analyzing drug targets for treating diseases.[23] The GO analysis revealed that the potential therapeutic targets of emodin are involved in 45 biological processes, including cellular response to hypoxia, response to xenobiotic stimulus, positive regulation of the apoptotic process, positive regulation of pri-miRNA transcription from RNA polymerase II promoter, extracellular matrix organization, positive regulation of fever generation, response to fructose, response to nematode, negative regulation of receptor activity, and negative regulation of lipid storage (Figure 4A). These targets are distributed across two main cellular components: membrane rafts and the extracellular matrix. These targets also involve ten molecular functions, including enzyme binding, transcription cofactor binding, identical protein binding, E-box binding, endopeptidase activity, peptidase activity, zinc ion binding, metalloendopeptidase activity, heme binding, and serine-type endopeptidase activity (Figure 4A). Based on the drug-target-pathway-disease analysis, we constructed a network comprising the top 15 KEGG pathways. The results suggest that emodin may alleviate PAH through one or more of these pathways (Figure 4B). Network pharmacology also highlighted the importance of eight hub genes: TNF, PTGS2, MMP1, MMP9, MYC, SLC2A4, CYP1A1, and PPARG (Figure 4B). Therefore, emodin may primarily inhibit the proliferation of PASMCs through the IL-17 signaling pathway, thereby alleviating PAH.

KEGG Enrichment and Molecular Docking Analysis

The experiment conducted KEGG enrichment analysis on the signaling pathways that may be involved in the alleviation of PAH by emodin. The results showed the top 15 signaling pathways (Figure 5A), among which the top 3 enriched pathways for the target genes are Lipid and atherosclerosis, IL-17 signaling pathway, and Pathways in cancer. In light of previous studies demonstrating a close association between the IL-17 signaling pathway and the onset and progression of PAH, we propose that this pathway may be the key mechanism by which emodin alleviates pulmonary arterial hypertension. The experiment also conducted molecular docking analysis on the binding of emodin to 8 targets of the IL-17 signaling pathway. Generally, ligand-receptor pairs with stable low-energy binding conformations have higher interaction possibilities.[8] The results showed that the key targets TNF, PTGS2, MMP1, MMP9, MYC, SLC2A4, CYP1A1, and PPARG had good binding with emodin, and the binding free energies were relatively low, ranging from −4.9 to −10.9 kcal/mol (Table 2). Among them, CYP1A1 had the lowest energy (−10.9 kcal/mol), followed by PTGS2 (−8.5 kcal/mol) and SLC2A4 (−8.5 kcal/mol). The visualization of molecular docking results showed the 8 pairs of emodin-combined target results (Figure 5B). The above results indicate that emodin may exert its therapeutic effects on PAH through interactions with multiple targets and pathways, with the IL-17 signaling pathway likely playing a crucial role.

Emodin Targets TAK1 to Inhibit IL-17 Signaling Pathway Activation

WB analysis was used to detect changes in the expression of key proteins in the IL-17 signaling pathway following emodin intervention. Results showed that compared to the control group, emodin intervention alone did not significantly affect the

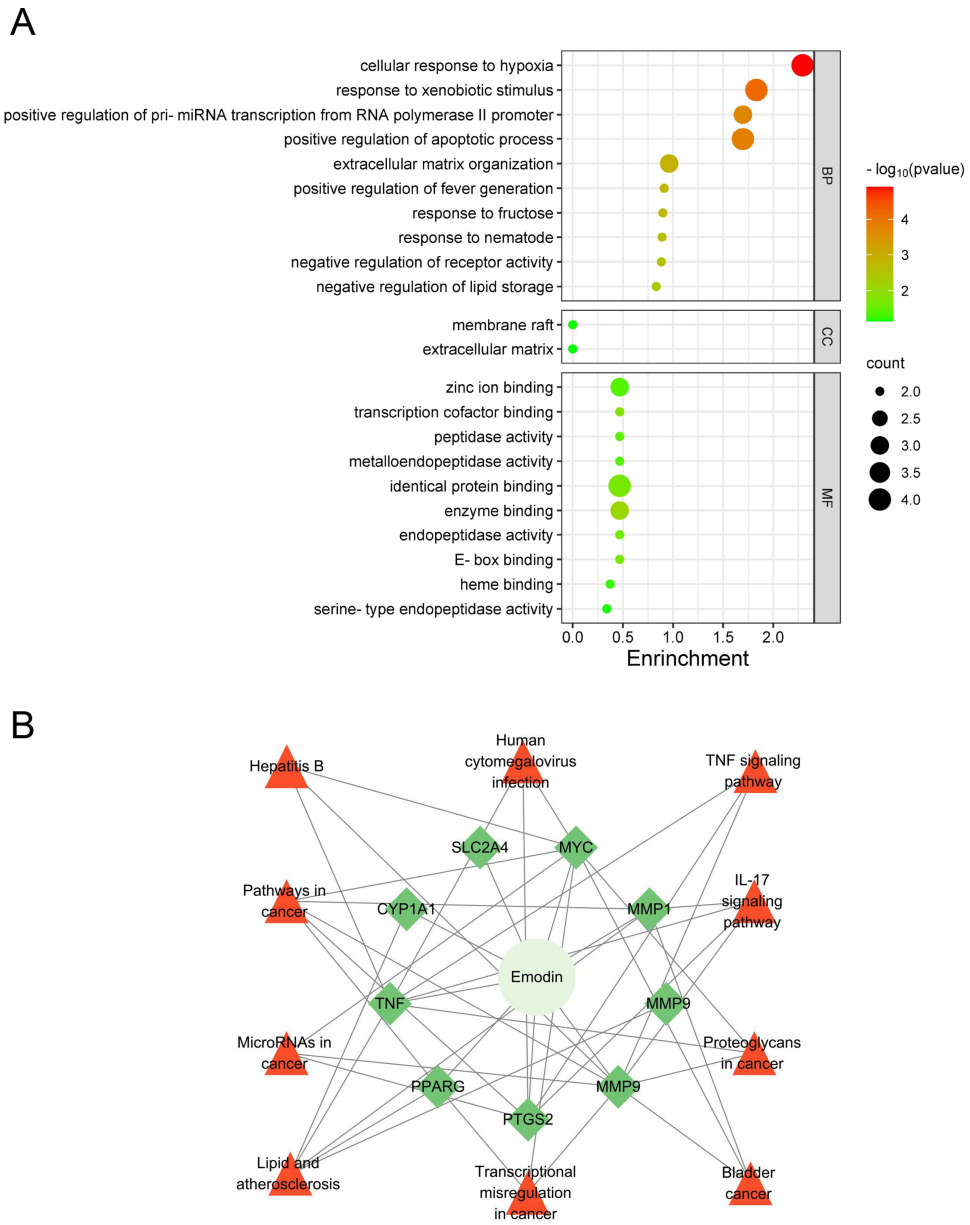

Figure 4 Network pharmacology analysis of the potential molecular mechanisms of emodin alleviating PAH. (**A**) Enrichment of overlapping targets. (**B**) Drug-target-pathway -disease map, red for drugs, blue for targets, green for pathways, and yellow for diseases.

IL-17 signaling pathway ($p > 0.05$). In the MCT group, compared to the control group, the expression of IL-17A and IL-17RA in lung tissue was significantly increased ($p < 0.05$), while the total expression of TAK1 showed no significant difference ($p > 0.05$). However, the expression of Phospho-TAK1 was significantly increased ($p < 0.01$). Compared to the MCT group, emodin significantly downregulated the expression of IL-17A ($p < 0.01$), IL-17RA ($p < 0.05$), and Phospho-TAK1 ($p < 0.01$), blocking the activation of the pathway (Figure 6A–E). Molecular docking demonstrated the binding of emodin to IL-17A, IL-17RA, and TAK1. The binding energies of IL-17A (−6.9 kcal/mol), IL-17RA (−6.4 kcal/mol), and TAK1 (−9.0 kcal/mol) with emodin were relatively low, suggesting that emodin might directly target these proteins. Among them, TAK1 had the lowest binding free energy (−9.0 kcal/mol), indicating that it is a primary target of emodin (Figure 6F–H). CETSA was used to verify the results of molecular docking.[24] Within a certain temperature range (40 °C - 65 °C), emodin intervention significantly increased the stability of IL-17A ($p < 0.05$), IL-17RA ($p < 0.05$), TAK1 ($p < 0.01$), and Phospho-TAK1 ($p < 0.01$). This indicates that emodin can directly bind to these proteins and maintain their structural stability. TAK1

https://doi.org/10.2147/DDDT.S540915

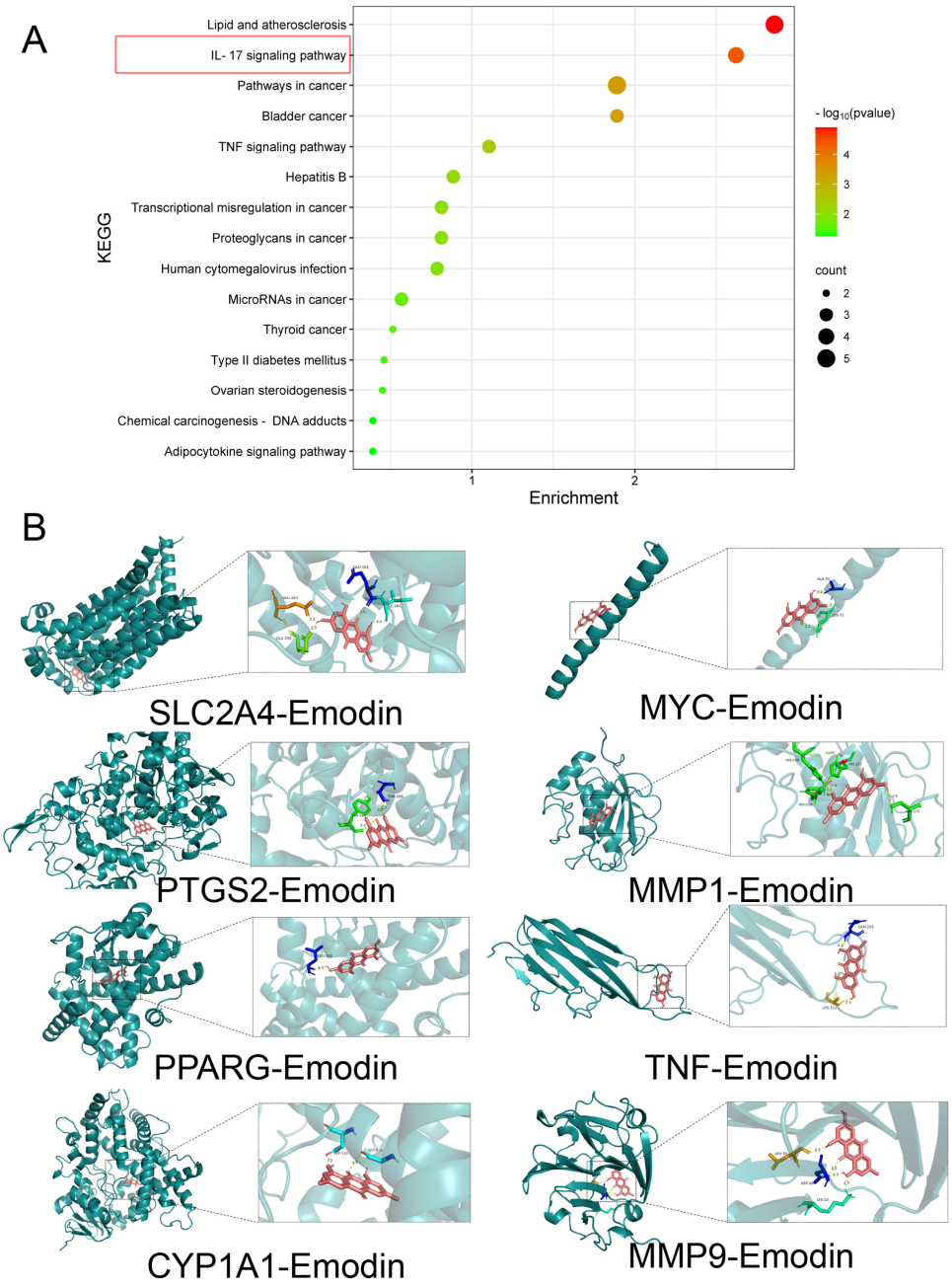

Figure 5 Results of KEGG enrichment and molecular docking. (**A**) KEGG enrichment analysis highlighting the top 15 signaling pathways potentially involved in the therapeutic effects of emodin on PAH. (**B**) Visualization results of molecular docking between 8 key components and emodin.

was identified as the main target of emodin (Figure 6I–M). These results confirm the potential of emodin as a TAK1-targeting inhibitor and provide strong support for its application in alleviating PAH.

Emodin Inhibits MCT-Induced Inflammatory Response

PCR results were consistent with WB. Emodin significantly downregulated the expression of IL-17A and IL-17RA genes ($p < 0.01$), while no significant difference was observed in TAK1 expression ($p > 0.05$) (Figure 7A). In addition, the detection of inflammatory factor expression in the lungs showed that emodin intervention in MCT-induced PAH significantly down-regulated the expression of IL-1β ($p < 0.01$), IL-6 ($p < 0.01$), and TNF-α ($p < 0.01$) (Figure 7A). These findings were further supported by changes in circulating inflammatory factors. ELISA results indicated that emodin intervention alone did not

Table 2 Binding Energy Between Selected Targets and Active Compounds

Molecule Name	Binding Energy (kcal/mol)
	Emodin
TNF	−6.9
PTGS2	−8.5
MMP9	−6.4
MMP1	−6.9
MYC	−4.9
SLC2A4	−8.5
CYP1A1	−10.9
PPARG	−8.3

induce significant circulating inflammatory responses compared to the control group ($p > 0.05$). In contrast, the MCT group exhibited significantly elevated levels of IL-1β, IL-6, and TNF-α compared to the control group ($p < 0.01$). Emodin intervention significantly inhibited the levels of IL-1β ($p < 0.01$), IL-6 ($p < 0.01$), and TNF-α ($p < 0.05$) (Figure 7B–D). These results suggest that emodin alleviates MCT-induced PAH by inhibiting inflammatory responses.

Emodin Inhibits Ang2-Induced Proliferation and Migration of PASMCs

Cell experiments were conducted to assess the effects of emodin on the migration and proliferation of PASMCs induced by Ang2.[25] The results showed that compared to the Ang2 group, emodin intervention for 24 hours significantly inhibited the migration of PASMCs ($p < 0.01$) (Figure 8A and B). The proliferation of cells in each group was detected at 24 hours and 48 hours. Compared to the control group, Ang2 significantly promoted the proliferation of PASMCs ($p < 0.01$). Emodin inhibited Ang2-induced proliferation in a concentration-dependent manner ($p < 0.01$) (Figure 8C and D). The results of PCNA staining were consistent with those of the CCK8 assay. Ang2 significantly promoted the expression of PCNA protein ($p < 0.01$), and emodin intervention could inhibit this expression ($p < 0.01$) (Figure 8E). TUNEL staining confirmed that compared to the Ang2 group, emodin intervention significantly promoted apoptosis in PASMCs ($p < 0.01$). This increased apoptosis may be an important mechanism by which emodin inhibits the proliferation of PASMCs.

Emodin Targets TAK1 to Regulate Its Activation and Signaling Transduction

The interaction between TAK1 and MKK3 was assessed via immunofluorescence colocalization following emodin treatment, which demonstrated that emodin intervention significantly reduced the interaction between TAK1 and MKK3 ($p < 0.05$) (Figure 9A). Co-immunoprecipitation assays further corroborated the aforementioned findings, Flag-tagged TAK1 was overexpressed in PASMCs, Co-immunoprecipitation experiments revealed that emodin significantly inhibited the binding of TAK1 to the MKK3 complex in a dose-dependent manner ($p < 0.05$) (Figure 9B and C). Additionally, in the presence of emodin, the phosphorylation levels of TAK1, JNK1/2, and p38 were significantly downregulated ($p < 0.05$) (Figure 9D and E). Similarly, the expression of inflammatory factors in cell lysates was assessed following emodin treatment. The results indicated that emodin significantly suppressed the expression of IL-1β, IL-6, and TNF-α ($p < 0.05$) (Figure 9F). Collectively, these findings suggest that emodin negatively regulates TAK1 activation and TAK1-dependent signal transduction pathways.

Emodin Targets TAK1 to Inhibit MCT-Induced PAH

Based on previous results, TAK1 was preliminarily identified as a key target of emodin's action. To further investigate the role of TAK1 in emodin's therapeutic effects, Takinib was used to inhibit TAK1 expression in rats with MCT-induced PAH. Ultrasound imaging revealed that compared to the MCT + Emodin group, Takinib intervention significantly reduced PAT and the PAT/PET ratio ($p < 0.05$) (Figure 10A–C). Additionally, mPAP was significantly upregulated

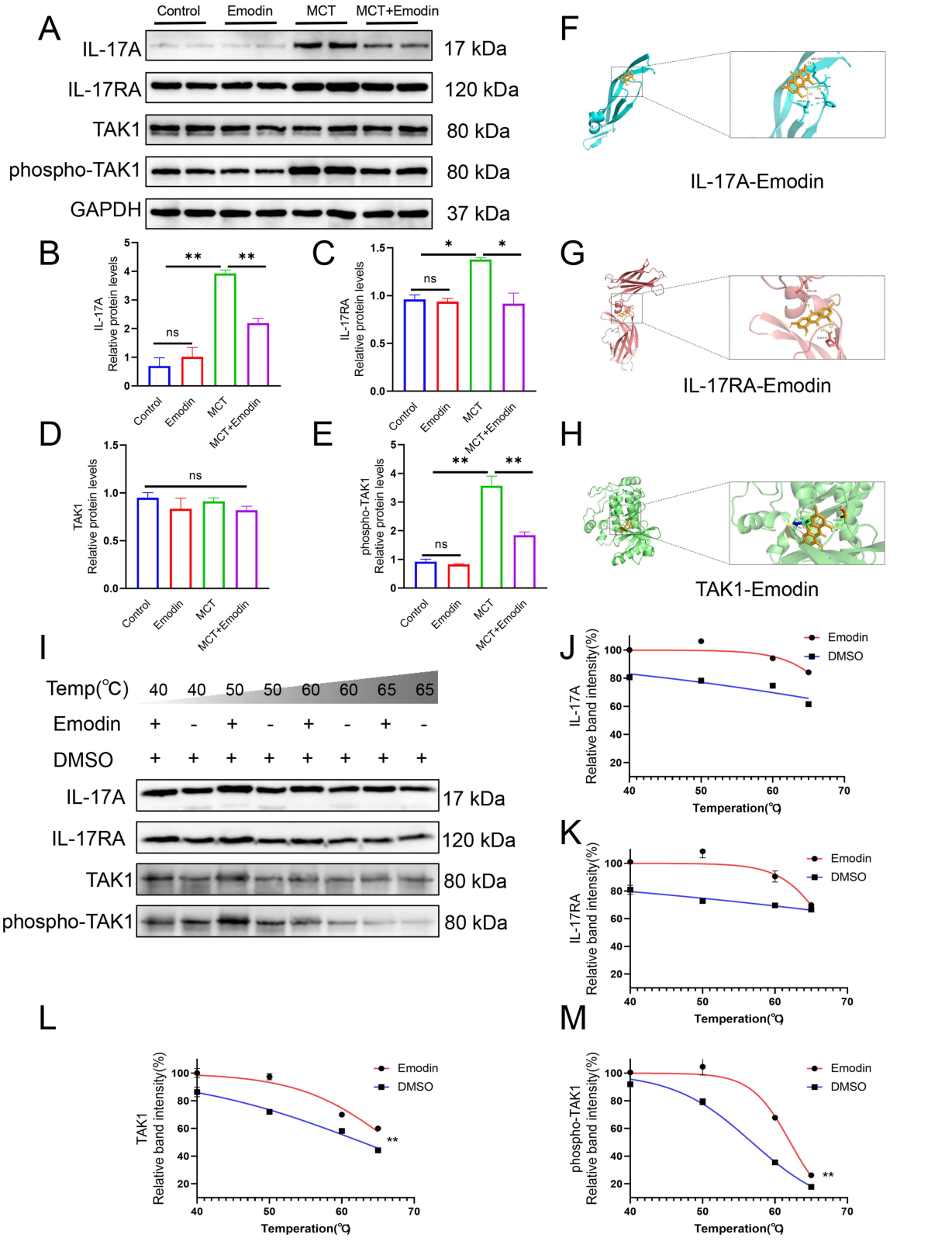

Figure 6 Emodin targets TAK1 to inhibit the activation of IL-17 signaling pathway. (**A**) WB analysis of the changes in key proteins of IL-17 signaling pathway in the lung of each group. The relative expression changes of IL-17A (**B**), IL-17RA (**C**), TAK1 (**D**), and Phospho-TAK1 (**E**) in each group. (**F**) Visualization results of the docking between IL-17A and emodin. (**G**) Visualization results of the docking between IL-17RA and emodin. (**H**) Visualization results of the docking between TAK1 and emodin. (**I**) CETSA verified the docking results. Statistical analysis of the differences in the stability of IL-17A (**J**), IL-17RA (**K**), TAK1 (**L**), and Phospho-TAK1 (**M**) after emodin intervention. The data are expressed as the mean ± standard deviation (±S).

Note: $^{**}p < 0.01$; $^{*}p < 0.05$; ns $p > 0.05$.

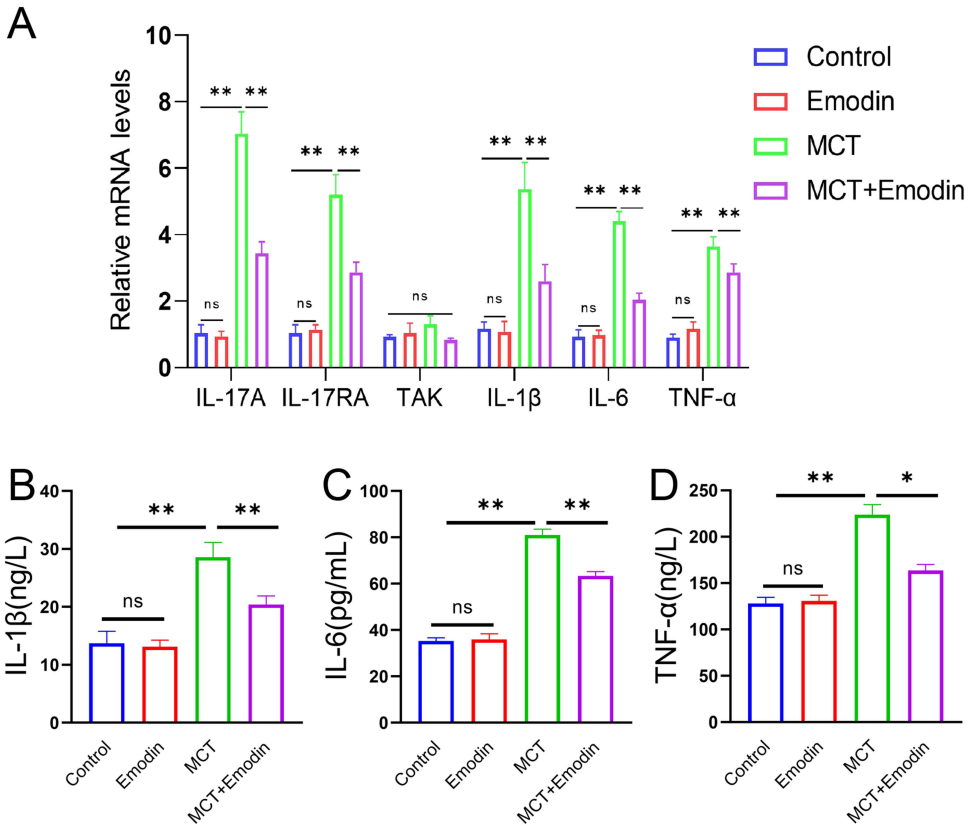

Figure 7 Emodin inhibits the inflammatory response induced by MCT. (**A**) PCR was used to detect the changes in gene expression of IL-17A, IL-17RA, TAK1, IL-1β, IL-6 and TNF-α in each group. ELISA was used to detect the changes in the contents of IL-1β (B), IL-6 (**C**) and TNF-α (**D**) in the serum of each group. The data are expressed as the mean ± standard deviation (±S).
Note: $^{**}p < 0.01$; $^{*}p < 0.05$; ns $p > 0.05$.

($p < 0.01$) (Figure 10D). The inhibitory effect of emodin on pulmonary artery wall thickening was also diminished by Takinib intervention (Figure 10E). Compared to the MCT + Emodin group, Takinib treatment increased inflammatory cell infiltration and significantly elevated the WT% ($p < 0.01$) (Figure 10F). α-SMA staining confirmed that after Takinib intervention, PASMCs regained their proliferative capacity (Figure 10G). Compared to the MCT + Emodin group, Takinib treatment significantly promoted the proliferation of PASMCs ($p < 0.05$), with proliferative activity similar to that of the MCT group ($p > 0.05$) (Figure 10H). These results confirm that Takinib significantly inhibited the therapeutic effects of emodin. Emodin inhibited the malignant proliferation of PASMCs by targeting TAK1, thereby alleviating MCT-induced PAH.

Discussion

PAH is a complex pathological process involving multiple factors, including inflammation, oxidative stress, and cell proliferation, which collectively contribute to the occurrence and progression of the disease.[26] The current treatment of PAH remains challenging. Previous studies have found that malignant smooth muscle proliferation leading to pulmonary artery stenosis is an important trigger for the development of PAH.[27,28] In this article, we have detailedly discussed the effects and mechanisms of emodin on PAH. For the first time, we discovered that emodin targets TAK1 and down-regulates the activation of the IL-17 signaling pathway. This significantly inhibits the proliferation of PASMCs induced by MCT and alleviates pulmonary inflammation and infiltration in the lungs, thereby alleviating PAH and right ventricular hypertrophy.

Emodin, named as "1,3,8-trihydroxy-6-methylanthraquinone" and with the molecular formula $C_{15}H_{10}O_5$, is a natural anthraquinone derivative extracted from Chinese herbal medicines such as rhubarb (Rheum palmatum), Japanese knotweed (Polygonum cuspidatum), and fleeceflower (Polygonum multiflorum). It has become a commonly used drug in

https://doi.org/10.2147/DDDT.S540915

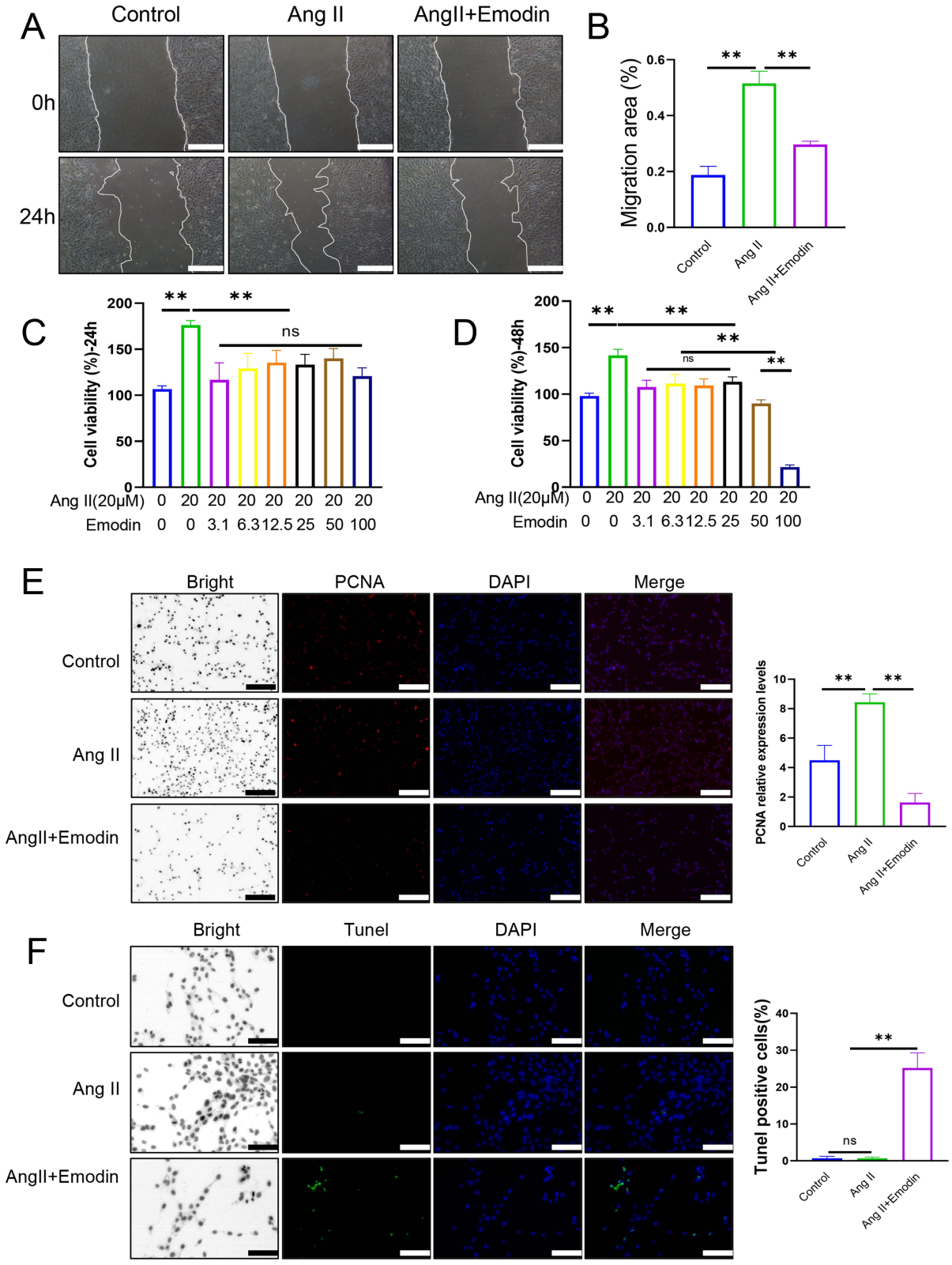

Figure 8 Emodin inhibits the proliferation and migration of PASMCs induced by Ang2. (**A**) Cell scratch assay to detect the effect of emodin on the migration of PASMCs induced by Ang2. (**B**) Statistical results of migration distance in each group. CCK8 assay to detect the effect of emodin on the proliferation of PASMCs induced by Ang2, respectively at 24h (**C**) and 48h (D). (**E**) Immunofluorescence to detect the changes in PCNA expression in each group. (**F**) Tunel staining to detect the changes in the proportion of apoptotic cells in each group. The data are expressed as the mean ± standard deviation (±S).
Note: $^{**}p < 0.01$; $^{*}p < 0.05$; ns $p > 0.05$.

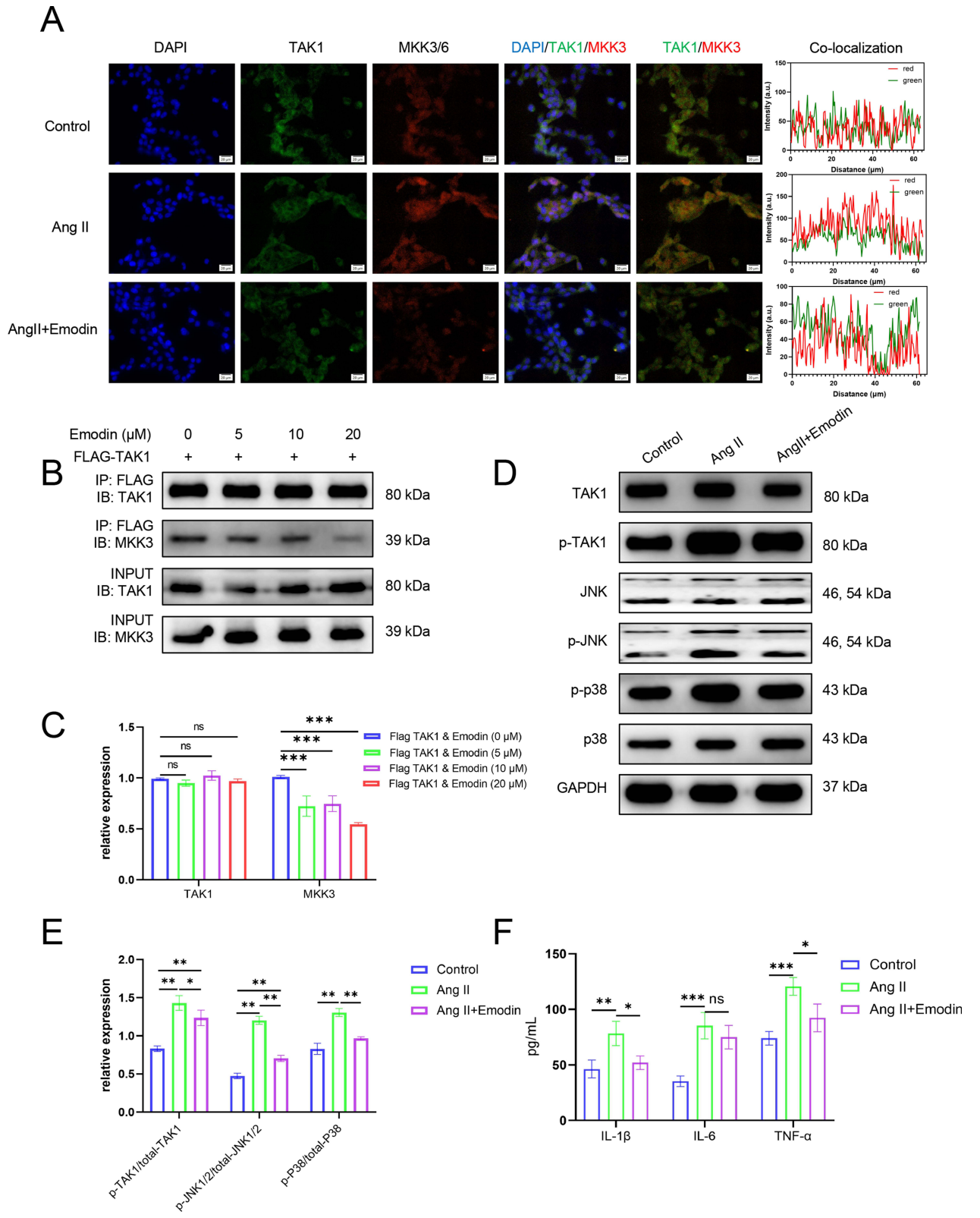

Figure 9 Emodin targets TAK1 to regulate its activation and signaling transduction. (**A**) Immunofluorescence microscopy was utilized to assess the co-localization of TAK1 and MKK3 after emodin intervention. (**B**) Co-immunoprecipitation assays were performed to investigate the alterations in the interaction between TAK1 and the MKK3 complex following emodin treatment. (**C**) Co-immunoprecipitation band intensities were quantified by densitometry. (**D**) Western blot analysis was employed to evaluate the activation status of downstream signaling pathways subsequent to emodin treatment. (**E**) Quantitative analysis of densitometric values was carried out for each experimental group. (**F**) ELISA was used to quantify the changes in the expression levels of IL-1β, IL-6, and TNF-α in cell lysates following emodin treatment. The data are expressed as the mean ± standard deviation (±S).
Note: ***$p < 0.001$; **$p < 0.01$; *$p < 0.05$; ns $p > 0.05$.

https://doi.org/10.2147/DDDT.S540915

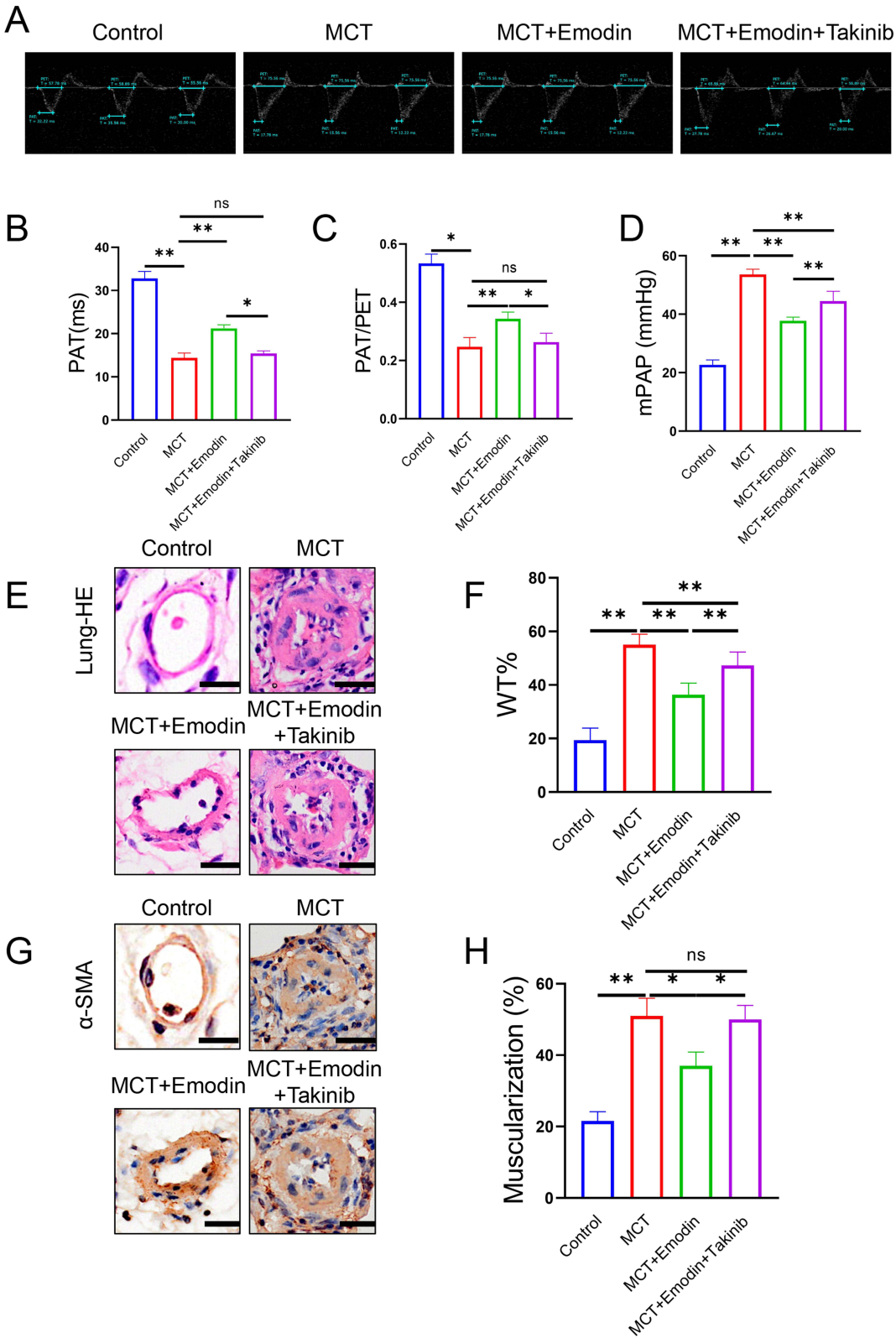

Figure 10 Emodin targets TAK1 to inhibit MCT-induced PAH. (**A**) Ultrasound measurement of changes in pulmonary artery blood flow velocity in each group. Changes in PAT (B), PAT/PET (**C**) and mPAP (**D**) in each group. (**E**) H&E examination of pathological changes in pulmonary arteries in each group. (**F**) Changes in WT% in each group. (**G**) Immunohistochemical labeling of pulmonary artery PASMCs. (**H**) Changes in Muscularization ratio in each group. The data are expressed as the mean ± standard deviation (±S).

Note: $^{**}p < 0.01$; $^{*}p < 0.05$; ns $p > 0.05$.

clinical practice and is included in the "Chinese Pharmacopoeia".[10] Previous in vitro experiments have confirmed that emodin can inhibit the proliferation of vascular smooth muscle cells.[29] Our research collective, in conjunction with prior investigations, has further substantiated that emodin mitigates vascular restenosis by inhibiting the proliferation of vascular smooth muscle cells.[30]

However, the role of emodin in PAH has not been fully elucidated. Previous reports have indicated that emodin can inhibit the viability, proliferation, and migration of PASMCs under hypoxic conditions by modulating the miR-244-5p-mediated DEGS1/PI3K/Akt signaling pathway and by promoting cell apoptosis.[13] Additionally, other studies have demonstrated that emodin inhibits TNF-α-induced proliferation of human aortic smooth muscle cells via caspase-dependent and mitochondrial apoptotic pathways.[12,31]

Our previous studies have demonstrated that emodin effectively inhibits vascular restenosis following balloon injury and exerts a significant inhibitory effect on the malignant proliferation of vascular smooth muscle cells.[30] These findings have been corroborated by other independent investigations. Additionally, it has been reported that emodin suppresses the proliferation of PASMCs following balloon injury by modulating the Wnt4/Dvl-1/β-catenin signaling pathway via miR-126.[30] Collectively, these results suggest that emodin may play a significant role in the treatment of PAH. In this study, we investigated the effects of emodin on MCT-induced PAH in rats. Our findings revealed that emodin significantly attenuated inflammatory cell infiltration in the lungs and markedly reduced the levels of IL-1β, IL-6, and TNF-α, which is consistent with the results of similar studies.[32,33] These observations further support the potential therapeutic application of emodin in the management of PAH. More importantly, emodin significantly inhibits the malignant proliferation of PASMCs, leading to a marked increase in the lumen size of small pulmonary arteries. Interestingly, emodin not only alleviates right ventricular hypertrophy (RVH) caused by PAH but also significantly improves myocardial remodeling.

Previous studies have shown that high-dose emodin increases the aggregation of block-like chromatin and lysosomes in VSMCs, thereby promoting apoptosis and autophagy.[29] Compared with endothelial cells, emodin exerts a more significant inhibitory effect on the proliferation of VSMCs.[11] Additionally, a concentration-dependent reduction in the expression of CDK1, Ki67, and E2F-1 genes in VSMCs has been observed following treatment with emodin.[11] Emodin also exhibits a significant inhibitory effect on the proliferation of VSMCs induced by angiotensin II.[14] The amplitude of the outward current in interlobar renal artery smooth muscle cells is enhanced in a concentration-dependent manner by emodin, thereby promoting relaxation of the interlobar arteries of the kidney.[34] These findings suggest that emodin may play a significant role in the development of PAH by influencing the function of PASMCs. This conjecture was confirmed by in vitro experiments, which demonstrated that emodin significantly inhibits the proliferation and migration of PASMCs and promotes apoptosis.

Through network pharmacology, we predicted that emodin might alleviate PAH by regulating the expression of key targets, including TNF, PTGS2, MMP1, MMP9, MYC, SLC2A4, CYP1A1, and PPARG. Molecular docking further confirmed this possibility, The eight target genes matched well with emodin. KEGG analysis revealed that the top 3 enriched pathways of the target genes were Lipid and atherosclerosis, IL-17 signaling pathway, and Pathways in cancer. In light of previous findings demonstrating a close association between the IL-17 signaling pathway and the onset and progression of PAH,[35] we hypothesize that the IL-17 signaling pathway may constitute the key mechanism by which emodin alleviates PAH. IL-17A, a key molecule in the IL-17 signaling pathway, has been confirmed as a pro-inflammatory factor involved in the occurrence and development of various immune diseases. Inhibiting the expression of IL-17A significantly alleviates inflammatory infiltration in PAH,[36] making it a promising target for early intervention in high-risk patients.[35]

To further verify the role of emodin in regulating IL-17 signaling pathway, we used CETSA to confirm the targeting of emodin on IL-17A, IL-17RA, TAK1, and Phospho-TAK1. Emodin demonstrates the most pronounced targeting effect on TAK1. TAK1 is a pivotal signaling protein that orchestrates the activation of multiple signaling pathways in response to growth factors, cytokines, and microbial products.[37] TAK1 has been confirmed as a key molecule involved in tissue inflammatory responses.[38] WB analysis revealed that emodin does not influence the expression levels of TAK1. This finding led us to hypothesize that emodin may inhibit the interaction of TAK1 with other proteins. Previous studies have established that the activation of TAK1 is tightly regulated by its binding partners and post-translational modifications.[39] Typically, the activation of TAK1 necessitates its association with MKK3, which subsequently modulates the activation

of downstream JNK/P38 signaling pathways.[40] Inhibiting the expression of TAK1 and Phospho-TAK1 significantly alleviates PAH.[41,42] In this study, we employed immunofluorescence and co-immunoprecipitation assays to elucidate the mechanism of action of emodin. Accumulating evidence indicates that MAPK cascades serve as a central hub integrating inflammatory and proliferative signals in PASMCs.[43] Upon pro-inflammatory stimulation, activated JNK, ERK, and p38 MAPK converge on the transcription factor AP-1. Phosphorylated AP-1 subsequently drives the transcription of IL-1β, IL-6, TNF-α, and other cytokines that promote PASMC proliferation.[44–46] Upstream of AP-1, TAK1 functions as the critical kinase that phosphorylates and activates the IKK complex (IKKα and IKKβ). Activated IKK complex then triggers IκBα degradation, enabling NF-κB nuclear translocation and transcriptional activation of pro-inflammatory and pro-proliferative genes.[47,48] Although our current findings strongly support that emodin suppresses NF-κB transcription by inhibiting TAK1 activation, future studies employing TAK1 knockout or NF-κB-specific inhibitors are warranted to definitively validate this pathway as the principal mechanism underlying the anti-inflammatory and anti-proliferative effects of emodin in PAH. Our results confirmed that emodin directly targets and binds to TAK1, thereby inhibiting the interaction between TAK1 and MKK3. This inhibition subsequently suppresses the activation of the downstream JNK/P38 signaling pathways. Consequently, a significant amelioration of cellular inflammation was observed. To further verify the role of emodin in the function of TAK1, we confirmed the above view by adding the TAK1 inhibitor (Takinib) in in vivo experiments.[49] Under the intervention of Takinib, the effect of emodin in alleviating PAH was significantly weakened, manifested as the recovery of PASMCs proliferation, narrowing of the pulmonary arterial lumen, increased infiltration of inflammatory cells in the lung, and recovery of pulmonary arterial pressure and pulmonary vascular remodeling to the level of simple MCT.

Our research still has some limitations. Due to the lack of specific drugs for PAH,[50] the experiments did not include positive control drugs. Additionally, the long-term side effects of emodin still need further study,[51] which will be the focus of our research group's next steps.

Conclusion

Based on the aforementioned findings, our study indicates that emodin alleviates MCT-induced PAH and significantly inhibits vascular remodeling. Through network pharmacology and molecular docking techniques, we identified the key pathways through which emodin exerts its therapeutic effects on PAH. The mechanism of action is primarily through targeting TAK1, inhibiting the activation of the IL-17 signaling pathway, and alleviating pulmonary inflammation and vascular remodeling. To our knowledge, this is the first study to elucidate the mechanism of emodin in treating PAH in vivo.

Data Sharing Statement

The data that supports the findings of this study are available on request from the corresponding author upon reasonable request.

Ethics Statement

The study was reviewed and approved by the Ethics Committee of The General Hospital of Western Theater Command (Approval No. 2025EC1-ky013).

Acknowledgments

We would like to show sincere appreciation to the reviewers for critical comments on this article.

Author Contributions

All authors made a significant contribution to the work reported, whether that is in the conception, study design, execution, acquisition of data, analysis and interpretation, or in all these areas; took part in drafting, revising or critically reviewing the article; gave final approval of the version to be published; have agreed on the journal to which the article has been submitted; and agree to be accountable for all aspects of the work.

Funding

This work was supported by Hospital Management Research of Western Theater General Hospital [2021-XZYG-C16], the Natural Science Foundation of Sichuan Province [2022NSFSC0822]. Traditional Chinese Medicine Research Program of Sichuan Provincial Administration of Traditional Chinese Medicine [25MSZX472].

Disclosure

The author(s) report no conflicts of interest in this work.

References

1. Xu Z, Ding J, Liang R, Xie S. Long-term trends in the burden of pulmonary arterial hypertension in China and worldwide: new insights based on GBD 2021. *Front Med*. 2024;11:1502916. doi:10.3389/fmed.2024.1502916
2. Mocumbi A, Humbert M, Saxena A, et al. Pulmonary hypertension. *Nat Rev Dis Primers*. 2024;10(1):1. doi:10.1038/s41572-023-00486-7
3. Ghofrani HA, Gomberg-Maitland M, Zhao L, Grimminger F. Mechanisms and treatment of pulmonary arterial hypertension. *Nat Rev Cardiol*. 2025;22(2):105–120. doi:10.1038/s41569-024-01064-4
4. Galie N, Brundage BH, Ghofrani HA, et al. Beardsworth A and others. Tadalafil therapy for pulmonary arterial hypertension. *Circulation*. 2009;119 (22):2894–2903. doi:10.1161/CIRCULATIONAHA.108.839274
5. Chen KH, Dasgupta A, Lin J, et al. Epigenetic dysregulation of the dynamin-related protein 1 binding partners MiD49 and MiD51 increases mitotic mitochondrial fission and promotes pulmonary arterial hypertension: mechanistic and therapeutic implications. *Circulation*. 2018;138(3):287–304. doi:10.1161/CIRCULATIONAHA.117.031258
6. Potus F, Pauciulo MW, Cook EK, et al. Novel mutations and decreased expression of the epigenetic regulator TET2 in pulmonary arterial hypertension. *Circulation*. 2020;141(24):1986–2000. doi:10.1161/CIRCULATIONAHA.119.044320
7. Liu J, Fang G, Lan C, et al. Forsythoside B mitigates monocrotaline-induced pulmonary arterial hypertension via blocking the NF-kappaB signaling pathway to attenuate vascular remodeling. *Drug Des Devel Ther*. 2024;18:767–780. doi:10.2147/DDDT.S444605
8. Chowdhury HM, Sharmin N, Yuzbasioglu BM, et al. BMPRII deficiency impairs apoptosis via the BMPRII-ALK1-BclX-mediated pathway in pulmonary arterial hypertension. *Hum Mol Genet*. 2019;28(13):2161–2173. doi:10.1093/hmg/ddz047
9. Wang XJ, Lian TY, Jiang X, et al. Germline BMP9 mutation causes idiopathic pulmonary arterial hypertension. *Eur Respir J*. 2019;53(3):1801609. doi:10.1183/13993003.01609-2018
10. Guo Y, Zhang R, Li W. Emodin in cardiovascular disease: the role and therapeutic potential. *Front Pharmacol*. 2022;13:1070567. doi:10.3389/fphar.2022.1070567
11. Xu K, Al-Ani MK, Wang C, et al. Emodin as a selective proliferative inhibitor of vascular smooth muscle cells versus endothelial cells suppress arterial intima formation. *Life Sci*. 2018;207:9–14. doi:10.1016/j.lfs.2018.05.042
12. Heo SK, Yun HJ, Park WH, Park SD. Emodin inhibits TNF-alpha-induced human aortic smooth-muscle cell proliferation via caspase- and mitochondrial-dependent apoptosis. *J Cell Biochem*. 2008;105(1):70–80. doi:10.1002/jcb.21805
13. Yi L, Liu J, Deng M, Zuo H, Li M. Emodin inhibits viability, proliferation and promotes apoptosis of hypoxic human pulmonary artery smooth muscle cells via targeting miR-244-5p/DEGS1 axis. *BMC Pulm Med*. 2021;21(1):252. doi:10.1186/s12890-021-01616-1
14. Wang S, Liu Y, Fan F, Yan J, Wang X, Chen J. Inhibitory effects of emodin on the proliferation of cultured rat vascular smooth muscle cell-induced by angiotensin II. *Phytother Res*. 2008;22(2):247–251. doi:10.1002/ptr.2301
15. Dong X, Fu J, Yin X, et al. Emodin: a review of its pharmacology, toxicity and pharmacokinetics. *Phytother Res*. 2016;30(8):1207–1218. doi:10.1002/ptr.5631
16. Xia T, Liang X, Liu CS, Hu YN, Luo ZY, Tan XM. Network pharmacology integrated with transcriptomics analysis reveals ermiao wan alleviates atopic dermatitis via suppressing MAPK and activating the EGFR/AKT signaling. *Drug Des Devel Ther*. 2022;16:4325–4341. doi:10.2147/DDDT.S384927
17. Xie W, Yang H, Guo C, Xie R, Yu G, Li Y. Integrated network pharmacology and experimental validation approach to investigate the mechanisms of stigmasterol in the treatment of rheumatoid arthritis. *Drug Des Devel Ther*. 2023;17:691–706. doi:10.2147/DDDT.S387570
18. Guo J, Yang ZC, Liu Y. Attenuating pulmonary hypertension by protecting the integrity of glycocalyx in rats model of pulmonary artery hypertension. *Inflammation*. 2019;42(6):1951–1956. doi:10.1007/s10753-019-01055-5
19. Liu HB, Yang M, Li W, et al. Dispelling dampness, relieving turbidity and dredging collaterals decoction, attenuates potassium oxonate-induced hyperuricemia in rat models. *Drug Des Devel Ther*. 2023;17:2287–2301. doi:10.2147/DDDT.S419130
20. Wang L, Moonen JR, Cao A, et al. Dysregulated smooth muscle cell BMPR2-ARRB2 axis causes pulmonary hypertension. *Circ Res*. 2023;132 (5):545–564. doi:10.1161/CIRCRESAHA.121.320541
21. Huang W, Zhou P, Zou X, Liu Y, Zhou L, Zhang Y. Emodin ameliorates myocardial fibrosis in mice by inactivating the ROS/PI3K/Akt/mTOR axis. *Clin Exp Hypertens*. 2024;46(1):2326022. doi:10.1080/10641963.2024.2326022
22. Rajaram SS, Desai NK, Kalra A, et al. Pulmonary artery catheters for adult patients in intensive care. *Cochrane Database Syst Rev*. 2013;2013(2): CD003408. doi:10.1002/14651858.CD003408.pub3
23. Yang HY, Liu ML, Luo P, Yao XS, Zhou H. Network pharmacology provides a systematic approach to understanding the treatment of ischemic heart diseases with traditional Chinese medicine. *Phytomedicine*. 2022;104:154268. doi:10.1016/j.phymed.2022.154268
24. Martinez MD, Jafari R, Ignatushchenko M, et al. Monitoring drug target engagement in cells and tissues using the cellular thermal shift assay. *Science*. 2013;341(6141):84–87. doi:10.1126/science.1233606
25. Ferguson BS, Wennersten SA, Demos-Davies KM, et al. DUSP5-mediated inhibition of smooth muscle cell proliferation suppresses pulmonary hypertension and right ventricular hypertrophy. *Am J Physiol Heart Circ Physiol*. 2021;321(2):H382–H389. doi:10.1152/ajpheart.00115.2021
26. Olsson KM, Corte TJ, Kamp JC, et al. Pulmonary hypertension associated with lung disease: new insights into pathomechanisms, diagnosis, and management. *Lancet Respir Med*. 2023;11(9):820–835. doi:10.1016/S2213-2600(23)00259-X

27. Lu X, Zhang J, Liu H, et al. Cannabidiol attenuates pulmonary arterial hypertension by improving vascular smooth muscle cells mitochondrial function. *Theranostics*. 2021;11(11):5267–5278. doi:10.7150/thno.55571
28. Shen H, Gao Y, Ge D, et al. BRCC3 regulation of ALK2 in vascular smooth muscle cells: implication in pulmonary hypertension. *Circulation*. 2024;150(2):132–150. doi:10.1161/CIRCULATIONAHA.123.066430
29. Wang X, Zou Y, Sun A, et al. Emodin induces growth arrest and death of human vascular smooth muscle cells through reactive oxygen species and p53. *J Cardiovasc Pharmacol*. 2007;49(5):253–260. doi:10.1097/FJC.0b013e318033dfb3
30. Hua JY, He YZ, Xu Y, Jiang XH, Ye W, Pan ZM. Emodin prevents intima thickness via Wnt4/Dvl-1/beta-catenin signaling pathway mediated by miR-126 in balloon-injured carotid artery rats. *Exp Mol Med*. 2015;47(6):e170. doi:10.1038/emm.2015.36
31. Meng L, Yan D, Xu W, Ma J, Chen B, Feng H. Emodin inhibits tumor necrosis factor-alpha-induced migration and inflammatory responses in rat aortic smooth muscle cells. *Int J Mol Med*. 2012;29(6):999–1006. doi:10.3892/ijmm.2012.940
32. Liu Y, Shang L, Zhou J, Pan G, Zhou F, Yang S. Emodin Attenuates LPS-induced acute lung injury by inhibiting NLRP3 inflammasome-dependent pyroptosis signaling pathway in vitro and in vivo. *Inflammation*. 2022;45(2):753–767. doi:10.1007/s10753-021-01581-1
33. Tian SL, Yang Y, Liu XL, Xu QB. Emodin attenuates bleomycin-induced pulmonary fibrosis via anti-inflammatory and anti-oxidative activities in rats. *Med Sci Monit*. 2018;24:1–10. doi:10.12659/MSM.905496
34. Zhang C, Xiao M, Cao N, et al. Emodin activates BK channel in vascular smooth muscle cells and relaxes the interlobar renal artery of rat. *Biomed Pharmacother*. 2022;153:113452.
35. Ono Y, Mogami A, Saito R, et al. Interleukin-17A is a potential therapeutic target predicted by proteomics for systemic sclerosis patients at high risk of pulmonary arterial hypertension. *Sci Rep*. 2024;14(1):29484. doi:10.1038/s41598-024-76987-6
36. Tang X, Wang C, Wang L, et al. Aureane-type sesquiterpene tetraketides as a novel class of immunomodulators with interleukin-17A inhibitory activity. *Acta Pharm Sin B*. 2023;13(9):3930–3944. doi:10.1016/j.apsb.2023.03.017
37. Ge B, Gram H, Di Padova F, et al. MAPKK-independent activation of p38alpha mediated by TAB1-dependent autophosphorylation of p38alpha. *Science*. 2002;295(5558):1291–1294. doi:10.1126/science.1067289
38. Wang Y, Huang G, Vogel P, Neale G, Reizis B, Chi H. Transforming growth factor beta-activated kinase 1 (TAK1)-dependent checkpoint in the survival of dendritic cells promotes immune homeostasis and function. *Proc Natl Acad Sci U S A*. 2012;109(6):E343–52. doi:10.1073/pnas.1115635109
39. Zeng JJ, Shi HQ, Ren FF, et al. Notoginsenoside R1 protects against myocardial ischemia/reperfusion injury in mice via suppressing TAK1-JNK/p38 signaling. *Acta Pharmacol Sin*. 2023;44(7):1366–1379. doi:10.1038/s41401-023-01057-y
40. Sakurai H, Miyoshi H, Mizukami J, Sugita T. Phosphorylation-dependent activation of TAK1 mitogen-activated protein kinase kinase kinase by TAB1. *FEBS Lett*. 2000;474(2–3):141–145.
41. Nasim MT, Ogo T, Chowdhury HM, et al. BMPR-II deficiency elicits pro-proliferative and anti-apoptotic responses through the activation of TGFbeta-TAK1-MAPK pathways in PAH. *Hum Mol Genet*. 2012;21(11):2548–2558. doi:10.1093/hmg/dds073
42. Yu M, Wu X, Wang J, et al. Paeoniflorin attenuates monocrotaline-induced pulmonary arterial hypertension in rats by suppressing TAK1-MAPK/NF-kappaB pathways. *Int J Med Sci*. 2022;19(4):681–694.
43. Tian H, Liu L, Wu Y, et al. Yang C and others. Resistin-like molecule beta acts as a mitogenic factor in hypoxic pulmonary hypertension via the Ca (2+)-dependent PI3K/Akt/mTOR and PKC/MAPK signaling pathways. *Respir Res*. 2021;22(1):8. doi:10.1186/s12931-020-01598-4
44. Grabiec AM, Korchynskyi O, Tak PP, Reedquist KA. Histone deacetylase inhibitors suppress rheumatoid arthritis fibroblast-like synoviocyte and macrophage IL-6 production by accelerating mRNA decay. *Ann Rheum Dis*. 2012;71(3):424–431. doi:10.1136/ard.2011.154211
45. Jin YJ, Ji Y, Jang YP, Choung SY. Acer tataricum subsp. ginnala inhibits skin photoaging via regulating MAPK/AP-1, NF-kappaB, and TGFbeta/Smad Signaling in UVB-irradiated human dermal fibroblasts. *Molecules*. 2021;26(3):662. doi:10.3390/molecules26030662
46. Xu Y, Lin L, Zheng H, et al. Protective effect of Amauroderma rugosum ethanol extract and its primary bioactive compound, ergosterol, against acute gastric ulcers based on LXR-mediated gastric mucus secretions. *Phytomedicine*. 2024;123:155236. doi:10.1016/j.phymed.2023.155236
47. Zhu G, Cheng Z, Huang Y, et al. TRAF6 promotes the progression and growth of colorectal cancer through nuclear shuttle regulation NF-kB/c-jun signaling pathway. *Life Sci*. 2019;235:116831. doi:10.1016/j.lfs.2019.116831
48. Reyes-Garcia J, Carbajal-Garcia A, Di Mise A, Zheng YM, Wang X, Wang YX. Important functions and molecular mechanisms of mitochondrial redox signaling in pulmonary hypertension. *Antioxidants*. 2022;11(3). doi:10.3390/antiox11030473
49. Shen H, Yuan J, Tong D, et al. Regulator of G protein signaling 16 restrains apoptosis in colorectal cancer through disrupting TRAF6-TAB2-TAK1-JNK/p38 MAPK signaling. *Cell Death Dis*. 2024;15(6):438. doi:10.1038/s41419-024-06803-6
50. Johnson S, Sommer N, Cox-Flaherty K, Weissmann N, Ventetuolo CE, Maron BA. Pulmonary hypertension: a contemporary review. *Am J Respir Crit Care Med*. 2023;208(5):528–548. doi:10.1164/rccm.202302-0327SO
51. Wang S, Fu JL, Hao HF, Jiao YN, Li PP, Han SY. Metabolic reprogramming by traditional Chinese medicine and its role in effective cancer therapy. *Pharmacol Res*. 2021;170:105728. doi:10.1016/j.phrs.2021.105728

Drug Design, Development and Therapy

Dovepress
Taylor & Francis Group

Publish your work in this journal

Drug Design, Development and Therapy is an international, peer-reviewed open-access journal that spans the spectrum of drug design and development through to clinical applications. Clinical outcomes, patient safety, and programs for the development and effective, safe, and sustained use of medicines are a feature of the journal, which has also been accepted for indexing on PubMed Central. The manuscript management system is completely online and includes a very quick and fair peer-review system, which is all easy to use. Visit http://www.dovepress.com/testimonials.php to read real quotes from published authors.

Submit your manuscript here: https://www.dovepress.com/drug-design-development-and-therapy-journal